

# 微量 Ca 元素对 AgCuZn 钎料性能的影响

鲍 丽<sup>1</sup>, 龙伟民<sup>1</sup>, 张冠星<sup>1</sup>, 隋方飞<sup>2</sup>, 李 浩<sup>2</sup>, 马 佳<sup>1</sup>

(1. 郑州机械研究所 新型钎焊材料与技术国家重点实验室, 郑州 450001;

2. 郑州大学 材料科学与工程学院, 郑州 450001)

**摘 要:** 洁净钢用钎料的洁净度应随洁净钢的发展不断提高, 为研究钎料在生产中引入的微量 Ca 元素影响, 以 BA45Cu30Zn 钎料为研究对象, 借助综合热分析仪、扫描电镜等手段, 分析了不同钙含量的钎料合金的熔化性能、微观组织以及铺展性能。结果表明, 随着 Ca 元素含量增加, 合金的固相线温度提高, 液相线温度降低, 固-液相线温度区间缩小; 钙以 CaO 晶核形式存在于合金组织中, 细化合金组织; Ca 元素的存在降低了合金钎料在 316LN 不锈钢上的铺展性能。

**关键词:** 微量 Ca 元素; AgCuZn 钎料; 熔化性; 微观组织; 铺展性能

**中图分类号:** TG425.2 **文献标识码:** A **文章编号:** 0253-360X(2012)12-0057-04



鲍 丽

## 0 序 言

对高质量不断增长的要求促使钢的洁净度不断提高, 从而避免由于夹杂物引起的问题, 可以明显改善钢材的力学性能和加工性能。为严格控制钢中的氧化物或硫化物夹杂物, 对不同用途的钢中夹杂物的尺寸和出现量都已有规定<sup>[1]</sup>。因此连接洁净钢所涉及到的焊接材料的纯度也应随着钢的洁净度提高提出更高的要求。银钎料是钎焊钢时使用最广泛的钎料<sup>[2]</sup>, 主要以 Ag-Cu-Zn 合金为基体。银铜锌三元系合金中含有  $\alpha$   $\beta$   $\gamma$   $\delta$   $\epsilon$   $\eta$  等相, 其中  $\alpha$ -Ag  $\alpha$ -Cu,  $\alpha$ -(Cu-Zn)  $\alpha$ -(Ag-Zn) 相具有良好的强度和塑性,  $\beta$  相是具有高强度中等塑性的相, 其余的都是脆性相, 因此需要优化合金成分使得钎料兼具强度高和塑性好的性能。

在银钎料的生产过程中, Ca 元素化学性质比较活泼而被引入合金中。关于 Ca 作为微量添加元素对不同合金系影响的报道已有不少。对于镁合金, 添加适量 Ca 元素能够提高起燃温度<sup>[3]</sup>、增强高温抗拉强度和屈服强度<sup>[4, 5]</sup>、抗氧化性和流动性<sup>[6, 7]</sup>以及耐腐蚀性<sup>[8]</sup>。陈位铭等人<sup>[9]</sup>研究了钙对灰铸铁组织和性能的影响, 认为钙在铁水中的溶解能力很差, 造渣倾向严重, 但能有效细化石墨组织, 提高材料性能。威尔逊<sup>[10]</sup>通过研究钙处理对钢的可焊性影响,

认为钙处理能提高 HY-80 钢的抗热裂性, 并且使钢的抗裂性得到较为恒定而显著的改善, 也能提高抗氢致冷裂性以及厚度方向塑性。然而 Ca 元素在银合金钎料中所起作用的数据甚少, 因此文中以 BA45Cu30Zn 钎料为研究对象, 研究 Ca 元素对银钎料的熔化性能、微观组织、润湿铺展等性能的影响, 以期生产钎焊钢的洁净钎料提供试验数据和理论依据。

## 1 试验方法

试验原料为金属银(纯度 99.95%)、铜(纯度 99.90%)、锌(纯度 99.99%)、钙(纯度 99.99%)。熔炼设备为中频炉, 首先在炉中熔炼成 AgCu 母合金, 然后按不同比例添加锌、钙, 熔炼成 (Ag45Cu30Zn)<sub>(1-x)</sub>Ca<sub>x</sub>(质量分数), 其中  $x$  值为 0, 0.001 5, 0.003, 0.005, 0.01, 0.05, 0.1。

采用 DSC(differential scanning calorimetry)技术分析不同钙含量银基合金钎料的熔化性能, 使用设备是由德国 NETZSCH 公司生产的型号 STA449F3 综合热分析仪。试验分析过程是在氮气保护气氛下的氧化铝坩埚内完成。根据 BA45Cu30Zn 合金钎料的熔化温度<sup>[11]</sup>, 对合金扫描的温度区间为 30 ~ 800 °C, 升温速率为 15 °C/min。扫描结果由 Proteus 软件分析。

根据钎料润湿性测定按照国家标准 GB/T 11364—2008《钎料润湿性试验方法》, 试验过程中

使用尺寸为 40 mm × 40 mm 的 316LN 不锈钢为母材, 钎焊温度为 770 °C, 保温 2 min, 室温下自然冷却后将润湿试件清洗干净, 将其与面积参照物一同扫描到计算机内, 用 AutoCAD 软件进行面积查询。

将合金钎料镶样, 然后用金相水砂纸打磨, 用 2.5 μm 的金刚砂抛光膏进行抛光, 最后用 4% 的 HNO<sub>3</sub> 酒精溶液腐蚀约 5 s, 制样完成。钎料合金微观组织结构在 JSM-7500F 扫描电镜分析仪检测, 不同区域组织的成分分布由 EDS (Oxford INCA-PentaFET-X3) 分析。

## 2 结果与分析

### 2.1 Ca 元素对 AgCuZn 钎料熔点的影响

不同 Ca 元素含量(质量分数)的合金钎料在扫描温度范围内的 DSC 曲线如图 1 所示。从图 1 中可知, 随着温度增加, 合金钎料发生相转变, 即由固相吸热转变为液相; 并且随着 Ca 元素含量的增加, 合金的吸热峰向右偏移。设定 DSC 曲线上吸热峰的起始点温度为合金的固相线点, 终止温度为液相线点<sup>[12]</sup>。根据图 1 得出各合金的吸热峰特征点, 列于表 1 中, 可以看出, Ca 元素含量增加, 合金的固相线温度的变化趋势为提高, 液相线温度的变化趋势为降低, 从而使得钎料的固-液相线温度区间减小。

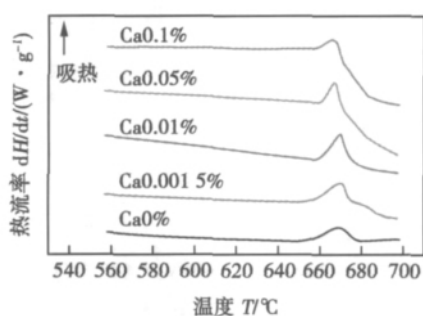


图 1 不同 Ca 元素含量 AgCuZn 合金的 DSC 分析曲线

Fig. 1 DSC curves of AgCuZn alloy with various calcium additions

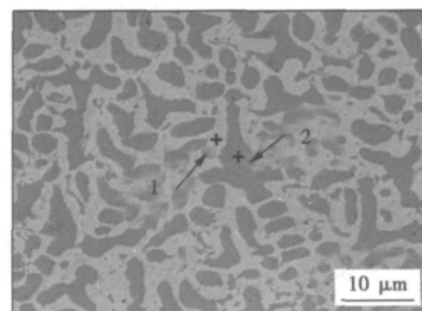
表 1 图 1 中吸热峰特征温度

Table 1 Characteristic temperature on endothermic peak in Fig. 1

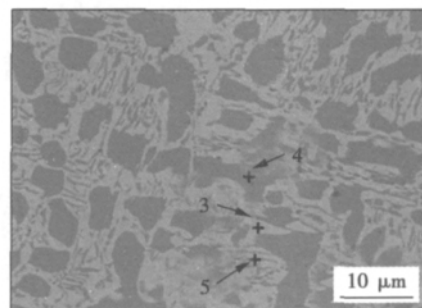
Ca 元素含量 $w(\%)$	熔化起始温度 $T_s/^\circ\text{C}$	峰值温度 $T_p/^\circ\text{C}$	熔化结束温度 $T_f/^\circ\text{C}$	固-液相线温 度区间 $\Delta T/^\circ\text{C}$
0	647	668.82	678	31
0.0015	650	669.9	679	29
0.01	656.5	669.71	683	26.5
0.05	659	666.66	673	14
0.1	657.5	664.04	669.5	12

### 2.2 Ca 元素对 AgCuZn 钎料微观组织的影响

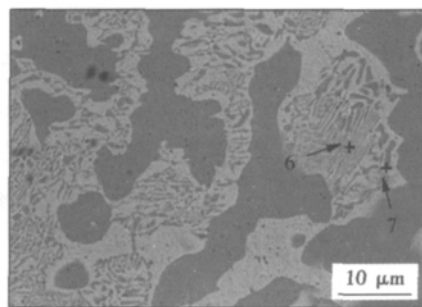
扫描分析仪检测添加不同 Ca 元素含量的 AgCuZn 钎料合金的微观组织结构变化如图 2 所示, 从图 2 中可以看出, 不同成分的合金组织具有相似的骨架。微观组织中特殊点的 EDS 能谱成分分析结果列于表 2, 由于 Ca 元素含量太低, 故没有检测到



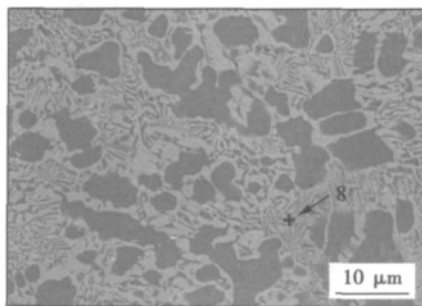
(a) Ca 元素含量 0.0015%



(b) Ca 元素含量 0.003%



(c) Ca 元素含量 0.01%



(d) Ca 元素含量 0.1%

图 2 AgCuZn 合金钎料的微观组织结构

Fig. 2 Microstructure of AgCuZn alloy varying with calcium addition

Ca 元素成分分布. 添加极少量 Ca 元素时(图 2a), 合金组织主要由  $\alpha$ -Ag 固溶体(灰色基体相)和铜基固溶体(黑色基体相)组成. 从点 1 的成分可知,  $\alpha$ -Ag 固溶体为银基铜锌固溶体, 强度和塑性较高. 铜基固溶体(点 2) 辅以 Cu-Zn 共晶成分, 含有少量 Ag-Zn 固溶体, 弥散分布在固溶体中. 当 Ca 元素添加量增大至 0.003% 时, 合金组织中除了灰色相和黑色相外, 还出现了条状组织, 如图 2b 所示, 其中点 3 和点 4 的成分分别与图 2a 中的点 1 和点 2 相近, 条状组织上点 5 成分为铜基固溶体, 但相对于黑色基体其 AgZn 固溶体含量相对高些. 因此认为由于 Ca 元素被氧化生成 CaO, 在冷却过程中合金组织以 CaO 为晶核, 在原有固溶体基相基础上生成了条状组织. Ca 元素含量继续增加, 就会有更多的 CaO 晶核形成, 析出的条状铜基固溶体的量增大, 如图 2c 所示, 从点 6 和点 7 的富铜相可以看出, 较细的条状组织(点 6) 比粗条状组织中(点 7) 的 AgZn 共晶成分高, 故析出相逐渐由条状转变为细纹状, 对晶体组织起到了细化作用. 当 AgCuZn 钎料中的 Ca 元素含量为 0.1% 时(图 2d), 细纹状组织已经均匀地弥散在银基固溶体和铜基固溶体之间, 其成分(点 8) 与点 6 相近.

表 2 图 2 中各点能谱成分分析(质量分数, %)

Table 2 Element content of spots in Fig. 2 analyzed by EDS

点	Cu	Zn	Ag
1	11.12	18.85	70.03
2	54.63	28.68	16.69
3	7.76	17.82	74.42
4	52.49	29.72	17.79
5	47.86	25.08	27.06
6	43.08	28.34	28.58
7	52.06	26.68	21.26
8	43.29	29.04	27.67

### 2.3 Ca 元素对 AgCuZn 钎料铺展性能的影响

银基钎料中 Ca 元素含量对钎料的润湿铺展性影响如图 3 所示. 随着 Ca 元素含量的增加铺展面积不断减小; 含量在 0.003% 以下时, 钎料铺展面积变化速率比较大, 在 0.003% 以上时, 铺展面积减小的速率变缓. 根据 2.1 的结果表明, Ca 元素含量越高, 合金的熔点越低. 报道认为实际液态金属都是粘性液体, 其流动性能可用液态金属的粘度来衡量, 粘度越大, 则流动性越差; 而粘度与液态金属的过热度成反比, 因此当钎焊温度一定时, 钎料的熔化温度

越低, 则液态钎料合金的过热度越大, 从而引起液态钎料合金的粘度降低, 流动性增强<sup>[13-15]</sup>. 但是对于含有 Ca 元素的 AgCuZn 钎料合金的铺展性能却与上述观点相悖. 分析 Ca 元素降低钎料与母材润湿性的主要原因可能是 Ca 元素比较活泼, 非常容易被氧化. 林高用等人<sup>[16]</sup>认为合金的熔体流动性与其抗氧化性也有着密切的联系, 抗氧化能力越强, 熔体流动性越好, Ca 元素的存在降低了合金的整体抗氧化性; 氧化物是很好的阻流剂材料, 使其在钢板铺展面积减小, 降低其与母材的润湿性. 因此应严格控制钎料中的 Ca 元素含量, 提高钎料本身与洁净钢母材的润湿性, 以便于形成良好的焊接接头.

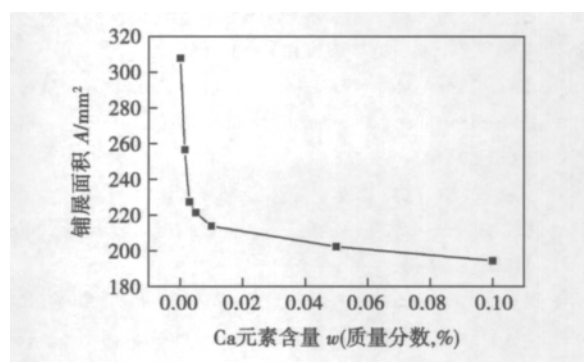


图 3 不同 Ca 元素含量 AgCuZn 钎料在 316LN 不锈钢上的铺展面积

Fig. 3 Spreading area of AgCuZn on 316LN stainless steel varies with calcium content

## 3 结 论

(1) Ca 元素含量增加, 合金钎料的 DSC 吸热峰向左偏移, 固相线温度升高, 液相线温度降低, 固-液相线温度区间缩小.

(2) Ca 元素以 CaO 形式存在于合金中, 并作为晶核, 使钎料基体组织中出现条状和细纹状组织, 细化合金组织.

(3) Ca 元素降低了合金的抗氧化性, 生成的 CaO 阻碍了合金钎料在 316LN 不锈钢上流动, 减弱了钎料的铺展性能.

### 参考文献:

- [1] Zhang Lifeng, Thomas B G. State of the art in evaluation and control of steel cleanliness [J]. ISIJ International, 2003, 43 (3): 271-291.
- [2] 张启运, 庄鸿寿. 钎焊手册 [M]. 北京: 机械工业出版社, 2008.

- [3] 蒋汉祥,郭 红,马立华,等. 加入钙和稀土对 AZ91D 镁合金起燃温度的影响[J]. 重庆科技学院学报(自然科学版), 2006, 8(2): 36-38.  
Jiang Hanxiang, Guo Hong, Ma Lihua, *et al.* Influence of adding RE and Ca on ignition temperature of AZ91D magnesium alloy[J]. Journal of Chongqing University of Science and Technology: Natural Science Edition, 2006, 8(2): 36-38.
- [4] 王 峰,刘 静,李晨曦,等. Ca-Y 合金化对压铸 AZ91 合金组织及性能的影响[C]//第十二届全国铸造年会暨 2011 中国铸造活动周论文集, 2011: 275-280.
- [5] 王利国,张宝丰,耿家源,等. 钙硅合金对 AM60 镁合金流动性的影响[J]. 铸造技术, 2005, 26(10): 927-929.  
Wang Ligu, Zhang Baofeng, Geng Jiayuan, *et al.* Effect of silico-calcium on the casting peroperties of AM60 alloy[J]. Foundry Technology, 2005, 26(10): 927-929.
- [6] 张亚琴,茂木彻一. 钙对 AZ91D 镁合金流动性的影响[J]. 机械工程材料, 2008, 32(10): 63-66.  
Zhang Yaqin, Motegi T. Effect of calcium on fluidity of AZ91D magnesium alloy [J]. Materials for Mechanical Engineering, 2008, 32(10): 63-66.
- [7] 张尧成,曾 明,廖春丽,等. 钙和硅元素对 AE41 镁合金显微组织及压入蠕变性能的影响[J]. 机械工程材料, 2009, 33(11): 50-54.  
Zhang Yaoheng, Zeng Ming, Liao Chunli, *et al.* Effect of Ca and Si on microstructure and indentation creep property of AE41 alloy[J]. Maetials for Mechanical Engineering, 2009, 33(11): 50-54.
- [8] 曹林锋,杜文博,苏学宽,等. Ca 合金化在镁合金中的作用[J]. 铸造技术, 2006, 27(2): 182-184.  
Cao Linfeng, Du Wenbo, Su Xuekuan, *et al.* Role of calcium alloying in magnesium alloys [J]. Foundry Technology, 2006, 27(2): 182-184.
- [9] 陈位铭,逢 伟,张继锋. 稀土、钙对灰铸铁组织和性能的影响[J]. 汽车工艺与材料, 2005(9): 8-11.  
Chen Weiming, Pang Wei, Zhang Jifeng. Effect of rare earth and calcium on gray iron structure [J]. Automobile Technology & Material, 2005(9): 8-11.
- [10] 威尔逊 R K. 钙和镁处理对钢的可焊性之影响[J]. 材料开发与应用, 1983(5): 8-16.  
Wilson R K. Influence of calcium and magnesium treatment on steel weldability [J]. Development and Application of Materials, 1983(5): 8-16.
- [11] 邹 僖. 钎焊[M]. 北京: 机械工业出版社, 1989.
- [12] 徐锦锋,张晓存,党 波. Ag-Cu-Sn 三元合金钎料的快速凝固组织与性能[J]. 焊接学报, 2011, 32(2): 85-88.  
Xu Jinfeng, Zhang Xiaocun, Dang Bo. Microstructure and properties of rapidly solidified Ag-Cu-Sn ternary brazing fillers [J]. Transactions of the China Welding Institution, 2011, 32(2): 85-88.
- [13] 卢方焱,薛松柏,张 亮,等. Ag-Cu-Zn 系钎料的研究现状及发展趋势[J]. 焊接, 2008(10): 13-19.  
Lu Fangyan, Xue Songbai, Zhang Liang, *et al.* Research status and prospect of Ag-Cu-Zn series brazing filler metals [J]. Welding & Joining, 2008(10): 13-19.
- [14] 卢方焱,薛松柏,张 亮,等. 微量 In 对 AgCuZn 钎料组织和性能的影响[J]. 焊接学报, 2008, 29(12): 85-88.  
Lu Fangyan, Xue Songbai, Zhang Liang, *et al.* Effect of trace indium on properties and microstructure of Ag-Cu-Zn filler metal [J]. Transactions of the China Welding Institution, 2008, 29(12): 85-88.
- [15] 马 力,龙伟民,乔培新,等. Zn-Mg 钎料钎焊镁合金 AZ31B 的显微组织与力学性能[J]. 焊接学报, 2011, 32(7): 59-62.  
Ma Li, Long Weimin, Qiao Peixin, *et al.* Microstructure and mechanical properties of magnesium alloy AZ31B solder joint using Zn-Mg filler metal [J]. Transactions of the China Welding Institution, 2011, 32(7): 59-62.
- [16] 林高用,彭大署,张 辉. AZ91D 镁合金锭的流动性研究[J]. 轻合金加工技术, 2001, 29(4): 16-17.  
Lin Gaoyong, Peng Dashu, Zhang Hui. Study on fluidity of AZ91D magnesium alloy ingots [J]. Light Alloy Fabrication Technology, 2001, 29(4): 16-17.

作者简介: 鲍 丽,女,1983 年出生,博士. 主要从事钎焊材料及焊接工艺方面研究. 发表论文 30 余篇. Email: baoli0222@yahoo.cn

通讯作者: 龙伟民,男,研究员,博士研究生导师. Email: brazelong@163.com

joint; filling weld

### Analysis and prevention of cracks in laser-welded joint of TiNi shape memory alloy and stainless steel

LI Hongmei<sup>1</sup>, SUN Daqian<sup>1</sup>, DONG Peng<sup>1</sup>, CAI Xiaolong<sup>2</sup> (1. School of Materials Science and Engineering, Jilin University, Changchun 130025, China; 2. State Key Laboratory of Rare Earth Resources Utilization, Changchun Institute of Applied Chemistry, Changchun 130022, China). pp 41–44

**Abstract:** Dissimilar metal joints of TiNi shape memory alloy wire and stainless steel wire were welded by laser welding method. The cracks feature and fracture surface morphology of joints were examined by using scanning electron microscopy (SEM) and confocal laser scanning microscope (CLSM). The mechanism of crack formation were analyzed, and some measurements were taken to control the welding cracks. The results showed that the micro-cracks usually emerged in the center of the weld zone and fusion zone of TiNi alloy side. The existence of a large number of brittle compounds in the weld was internal cause of cracks, and the joint subjected to tensile stress was the necessary condition of cracks. The cracking susceptibility can be improved to a certain extent by adding Ni interlayer, Co interlayer, changing the laser beam position, applying an axial force to weld zone and optimizing the laser welding parameters. Adding metal interlayer was a more effective method. The tensile strength reached 372 MPa and 347 MPa respectively by using Ni and Co interlayer, and the joint strength increased by 98.9% and 85.6% respectively, compared with the joint without metal interlayer.

**Key words:** TiNi shape memory alloy wire; stainless steel wire; laser welding; cracks

### Experimental analysis on fusion ratio and composition uniformity of laser hot wire welds

ZHENG Shiqing<sup>1</sup>, WEN Peng<sup>1,2</sup>, SHAN Jiguo<sup>1,2</sup> (1. Department of Mechanical Engineering, Tsinghua University, Beijing 100084, China; 2. Key Lab for Advanced Materials Processing Technology, Ministry of Education, Beijing 100084, China). pp 45–48, 72

**Abstract:** Ductile cast iron is welded with filling stainless steel hot wire in this article, then fusion ratio and distribution of elements are studied. The fusion ratio is as low as 38%–55%. The composition of filler wire distributes in welds uniformly. Nonuniform degrees of element Cr and Ni are 0.5% and 6%. Compared with laser hot wire welding, the fusion ratio of laser-MIG hybrid welds is 69%–77%, and the nonuniform degrees of element Cr and Ni are not less than 62% and 51%. The low electric energy input and its high utilization ratio for heating filler wire contribute to lower fusion ratio in laser hot wire welding compared to laser-MIG hybrid welding. The uniform distribution of filler wire in laser hot wire welds results from the low fusion ratio and solid filler wire transfer.

**Key words:** laser hot wire welding; laser-MIG hybrid welding; fusion ratio; distribution of elements; ductile cast iron

### Joint microstructure and isothermal solidification modeling during transient liquid-phase bonding of a duplex stainless steel

YUAN Xinjian<sup>1</sup>, LUO Jun<sup>1</sup>, TANG Kunlun<sup>1</sup>, LI Jia<sup>1</sup>,

KANG Chungyun<sup>2</sup> (1. College of Materials Science and Engineering, Chongqing University, Chongqing 400044, China; 2. Department of Materials Science and Engineering, Pusan National University, Busan 609735, Korea). pp 49–52

**Abstract:** An experimental investigation on transient liquid-phase bonding of a duplex stainless steel was carried by using Ni-based amorphous alloy as the interlayer. The microstructure of the bonded joint was observed with field emission scanning electron microscope (FE-SEM). The chemical compositions were analyzed by energy-dispersive X-ray spectroscopy (EDS) and wavelength-dispersive spectrometry (WDS). Phase structure of the bonded joint was identified by using X-ray diffraction (XRD). The results indicated that before the completion of isothermal solidification, the major secondary-phase precipitate present in the interface region between the insert and base alloy was BN. The dominating phases appeared in the interlayer zone were  $\gamma$ -Ni solid solution,  $\text{Ni}_3\text{B}$  and Cr-borides. Additionally, three diffusion models were employed to calculate the completion time of the isothermal solidification. By contrast to experimental results, the value obtained by solute distribution model was close to the actual value, and this model was considered to be suitable to the bonding process.

**Key words:** duplex stainless steel; Ni-based amorphous alloy; transient liquid-phase; microstructure; isothermal solidification

### Affecting factors of forming spiking of titanium alloy electron beam deep penetration welding

SHI Mingxiao<sup>1</sup>, ZHANG Binggang<sup>2</sup>, MA Jilong<sup>2</sup>, CHEN Guoqing<sup>2</sup>, FENG Jicai<sup>2</sup>, FAN Ding<sup>1</sup> (1. State Key Laboratory of Gansu Advanced Non-ferrous Metal Materials, Lanzhou University of Technology, Lanzhou 730050, China; 2. State Key Laboratory of Advanced Welding and Joining, Harbin Institute of Technology, Harbin 150001, China). pp 53–56

**Abstract:** The spiking is the unique defect of electron beam welding, which has a serious impact on the welding quality. The academia still hadn't had an unified understanding of the forming mechanism of spiking. To study the forming mechanism of spiking, the orthogonal test was used to carry out the experiment of titanium alloy electron-beam deep-penetration welding. The X-ray detection was done for each weld after welding. The results of X-ray detection show that the spiking only exists in the partial penetration weld, and the spiking is the irregular-slited shape while the roots are round. The optical microscope and scanning electron microscope combined with energy dispersion spectroscopy were used to analyze the formation mechanism of spiking. The results show that the pulse of electron beam is the direct cause of spiking formation and the metal vapor with high saturated vapor pressure accelerates the tendency of forming spiking. It is important intrinsic motivation to the generation of spiking.

**Key words:** electron beam welding; metal vapor; spiking

### Effect of trace calcium on performance of AgCuZn alloy

BAO Li<sup>1</sup>, LONG Weimin<sup>1</sup>, ZHANG Guanxing<sup>1</sup>, SUI Fangfei<sup>2</sup>, LI Hao<sup>2</sup>, MA Jia<sup>2</sup> (1. State Key Laboratory of Advanced Brazing Filler Metals and Technology, Zhengzhou Institute of

Mechanical Engineering , Zhengzhou 450001 , China; 2. School of Material Science and Engineering , Zhengzhou University , Zhengzhou 450001 , China) . pp 57 – 60

**Abstract:** The purity of the brazing alloys is necessary to be improved with the increasing cleanness of steel. This paper aims at investigating the influence of trace calcium that is contained in filler metal during production process. The melting property , microstructure and spreading performance of BAg45Cu30Zn alloy with various calcium additions have been studied , by employing simultaneous thermal analyzer and scanning electron microscope. The results show that the solidus temperature increases , the liquidus temperature decreases and the melting range narrows , with the calcium content increasing in alloy. The element calcium in the form of CaO exists as the crystal nucleus to refine alloy microstructure. The spreading performance of alloy on 316LN stainless steel has been weakened , resulting from the existence of calcium element.

**Key words:** trace calcium; AgCuZn brazing alloy; melting property; microstructure; spreading performance

**Microstructure and mechanical behaviors of stainless steel weld metal by ultrasonic assisted pulse TIG welding technology** ZHANG Qinlian , LIN Sanbao , FAN Chenglei , YANG Chunli ( State Key Laboratory of Advanced Welding and Joining , Harbin Institute of Technology , Harbin 150001 , China) . pp 61 – 64

**Abstract:** Ultrasonic assisted TIG welding is a new technology with high efficiency. In previous study , direct current was used. However , pulse current was expected in actual welding production. In this study , ultrasonic assisted pulse TIG welding technology was applied to weld 1Cr18Ni9Ti austenitic stainless steel. Microstructure and mechanical properties of the joints were analyzed. The reasons for weld penetration increasing and microstructure refinement were discussed. Experimental results indicated that the welding penetration with ultrasonic vibration was double of that without it. The microstructure of the weld zone was refined and the arc shape was compressed in base current period. The ultimate tensile strength and elongation were higher than that without ultrasonic vibration. Weld penetration increasing is perhaps attributed to acoustic streaming as the main driving force. The refinement of microstructure may be caused by the corporate effects of acoustic cavitation and acoustic streaming.

**Key words:** stainless steel; ultrasonic vibration; grain refinement; mechanical property

**Study on life-prediction of solder joint under combined loading** WANG Huan , YANG Ping , XIE Fangwei , XI Tao ( School of Mechanical Engineering , Jiangsu University , Zhenjiang 212013 , China) . pp 65 – 68

**Abstract:** A life-prediction approach of solder joints under combined thermal and vibration loading is provided in this paper. The deformations of solder joints are calculated respectively under vibration and thermal cycling loading based on finite element method. The calculated results are defined as boundary conditions of the multiaxial loading to investigate the strain/stress of the solder joints. Then the life of solder joints is calculated. The result reveals that the life of solder joints can be divided into

three regions according to the vibration amplitude at the same temperature: the life of solder joints in region I is affected by thermal loading; that in region II is greatly affected by the combined loading; that in region III is affected by the vibration amplitude. The trend of the simulation results basically agrees with that of the test results.

**Key words:** solder joints; combined loading; life-prediction

**Analysis for microstructure and mechanical property of Sn-3Ag-0.5Cu solder joints in high density LED packages**

WANG Xinxin<sup>1</sup> , LIU Jianping<sup>1</sup> , GUO Fu<sup>1</sup> , LIU Li<sup>2</sup> , LEI Yuanhong<sup>2</sup> ( 1. College of Materials Science and Engineering , Beijing University of Technology , Beijing 100124 , China; 2. R&D Center , Beijing Leyard Electronic Science Technology Co. , Ltd , Beijing 100091 , China) . pp 69 – 72

**Abstract:** The microstructure of Sn37Pb and Sn3Ag0.5Cu solder joints under as-reflowed and isothermal aged conditions were observed respectively. The shear strength of samples were also measured. The results suggested that despite the IMC layer of the Sn37Pb solder joints was thicker than the Sn3Ag0.5Cu solder joints , both of them were within the acceptable range. The Sn3Ag0.5Cu solder joints shows a bigger shear strength due to its special structure of  $\beta$ -Sn primary crystal coated by reticular eutectic. Besides , the shear strength of the two solder joints decreased after aging. Although lead-free solder is the inevitable trend to the development of electronic packaging industry instead of Sn37Pb solder , precision reflowing process still plays an important role to improve the quality of the solder joints.

**Key words:** LED package; eutectic solder alloys; microstructure; shear strength

**Spectrum analysis of A-TIG welding for aluminum alloy**

YAN Keng<sup>1</sup> , YANG Gang<sup>1</sup> , ZHAO Yong<sup>1</sup> , GAO Lihua<sup>1</sup> , LU Jiansheng<sup>2</sup> ( 1. Provincial Key Lab of Advanced Welding Technology , Jiangsu University of Science Technology , Zhenjiang 212003 , China; 2. Shanghai Waigaoqiao Shipbuilding Co. , Ltd , Shanghai 200137 , China) . pp 73 – 76 , 105

**Abstract:** A-TIG welding experiments were conducted by using five species of single-component activating fluxes , including SiO<sub>2</sub> , TiO<sub>2</sub> , CaF<sub>2</sub> , Cr<sub>2</sub>O<sub>3</sub> , BaCl<sub>2</sub> and complex formulation YG304. The spectrum in A-TIG welding process is tested by spectrometer. The distribution law of flux element in arc space is analyzed. The experimental results indicate that the above activating fluxes have different effects on weld penetration. The most remarkable increasing is obtained when the flux is YG304. The spectral lines of argon atom and aluminum atom are the main spectral lines of the A-TIG welding arc. Different cross-spectrum distribution of arc is presented with different fluxes. The increasing of penetration may be attributed to the recombination of positive ions such as Si<sup>4+</sup> , Ti<sup>4+</sup> , Cr<sup>3+</sup> and electron that generates from Ar arc , thus raise the arc temperature and arc force , and ultimately the weld penetration increases. The effect of increased penetration is due to various physical properties of positive ion.

**Key words:** aluminum alloy; A-TIG; cross-spectrum; weld penetration